BALLISTIC FLIGHT AND CONTROL SIMULATION OF RKX200TJ/BOOSTER DURING BOOST AND CLIMB-PHASES

Hakiki
Rocket Technology Center, LAPAN
e-mail: haqq.lapan@gmail.com
Received: 7 October 2020; Revision: 11 November 2020; Accepted: 11 November 2020

ABSTRACT

The problem encountered while developing the RKX-200TJ/booster is the measurement of vehicle mass (center of gravity). The thrust line of the rocket booster does not coincide with the center of gravity can induce a pitch disturbance. By controlling the pitch parameter, the pitch disturbance phenomenon can be minimized. In this paper presents the flight performance and dynamics analysis and the design of the pitch and roll control system for RKX200TJ/booster during rocket boost and climb phase. The result indicates that the pitch disturbance can be reduced until 27% decrease whereas roll angle (ϕ) can be damped at zero level ($\phi = 0$). Pitch angle (θ) can be maintained at angle 5° for the climb phase. Although the one of moment arm case shows the static instability and uncontrollability during rocket boost phase, the control system can control the vehicle to further phase. This simulation is presented in X-Plane and Simulink. The PID controller is selected in the control system design.

Keywords: *PID controller, RKX200TJ/booster, rocket booster, X-Plane, Simulink.*

1 Introduction

The development of unmanned aerial vehicle (UAV) technology has been growth more progress, such as the variantions of configuration form, advances in electronic system devices and increased thrust engine power. UAVs are commonly categorized into three groups based on configuration, capability and flight mission, namely fixed-wing UAVs, rotary-wing UAVs, and Hybrid UAVs (R. Austin, 2010). In the last decade, as several small industries and hobbies have made UAV known as drones, so that researchers or academics who working in the field of system devices often use them as a vehicle to develop their avionics systems.

Researchers or engineers have been conducting experiments to develop the concept of a short take-off in UAV in the last decade, although this concept has emerged a long time ago. The main idea of the concept is that the UAV can be launched in a catapult or booster environment. The last type is an assistance take-off device to assist the vehicle by providing an additional small rocket boost. This type can be used anywhere, even on the ships because it does not require a runway (Hakiki, 2020).

Rocket Technology Center (Pustek Roket) still develops the UAV technology, in particular the control system. The control system used is software and hardware system which have an open-source research platform enable full onboard processing on a micro air vehicle (Lorenz, *et al.*, 2011). This control system has been applied on high subsonic speed vehicle and it works but there are still inaccuracy. Based on several experience in testing, it is

necessary to research independent control system further.

RKX-200TJ/booster is an designed unmanned aerial vehicle (UAV) flies at speed 200 – 250 km/h and can be used to the telemetry control system testing (Satrya, *et al.*, 2014). The vehicle has not landing gear for take-off dan landing. The vehicle uses pneumatic launcher for take-off (Hakiki and Edi Sofyan, 2013), besides a single rocket booster. Whereas the second thrust using jet engine for cruise phase of flight.

Previously, several studies have been published concerning the RKX200 vehicle, in regarding to design, simulation, measurement and manufacturing. Riyadl in (Riyadl, 2015) researched the effect of moments on the flight dynamics of the RKX-200TJ/booster to determine the optimal moment distance so that the vehicle can fly quite stable during take-off phase. During take-off phase by using booster rocket, there are the change in aerodynamic forces and the shift of vehicle's center of mass. The shift of the mass center will result in a moment force on the vehicle because of the booster thrust, (Riyadl and Hakiki, 2014). In this case is not explained how the control system is applied on vehicle so that the vehicle can fly adequately stable in spite of disturbance occurrence. Shandi *et al.*, predicted the location of the center of gravity of the RKX200TJ/booster. The center of gravity (CG) prediction based on mathematical calculations. The calculation is done by knowing the weight of each component of the vehicle and then calculating its effect on the vehicle's center of gravity. Calculations are carried on in the X-axis direction (X_{CG} abscissa point) and Z-axis direction (Z_{CG} ordinate point) in two flight conditions, namely take-off phase and the rocket booster is burned out. (Shandi and Hakiki, 2016). Shandi *et al.*, only performed the CG calculations and did not discussed the flight performance dan dynamics. This calculation provided a reference for other further designs. Meanwhile, Bo Liu *et al.*, analyzed the take-off process on UAVs with a single rocket booster. Modeling is done using ANSYS, wind tunnel testing, and empirical calculations. Simulations were performed by varying the booster angle deviation longitudinally and laterally (Liu, *et al.*, 2011) instead of the moment arm in their paper. Once the single rocket booster has burned out, the velocity of UAV decreased. So, the designed control system was less effective.

Riyadl explained the occurrence of a wobbling movement on a ballistic rocket. This phenomenon can occur because the point of the rocket's center of mass which is not located on the symmetry axis of the rocket. The asymmetry of the center of mass causes disturbance in the roll, pitch and yaw moments on the rocket, where the perturbation of the roll, pitch and yaw moments triggers the wobbling motion (Riyadl, *2015*). The asymmetry effect of the rocket itself is taken into consideration in the control system design of RKX-200TJ/booster.

Based on the above background, this paper analyzes the pitching moment effect of the RKX-200TJ/booster in terms of flight performance and stability, and then carried on the pitch and roll control system design for rocket booster and climb phases so that the vehicle flies stable.

2 Methodology

The line of force of the rocket booster usually passes through the center of the vehicle's mass (center of gravity, CG) in ideal conditions. In real condition, this is not a fact. This problem often occur a

measurement error. The misalignment of the rocket's propulsion line to the CG point generates a moment arm (d_{arm}) so that it affects the stability and its flight path. If the CG point lies above the thrust line, it will cause a pitch-up moment, as shown in Figure 2-1 (a). Otherwise, if the point CG lies below the thrust line, it will cause a pitch-down moment, as shown in Figure 2-1 (b). In this case, the point CG is assumed to lie only in the direction of the longitudinal axis and the vertical axis of the vehicle.

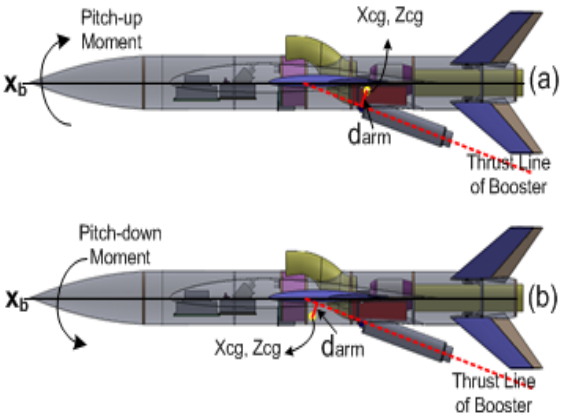

Figure 2-1: Illustrates the pitch effect

The aircraft model is simulated in X-plane in which the characteristics of aerodynamic can be used to predict the flying qualities. So, the block aircraft dynamics is replaced by the flight simulator X-plane (Kaviyarasu and Senthil, 2014), whereas the control system design is presented in Simulink, as shown in Figure 2-2. The UDP (*User Datagram Protocol*) communication is built between Simulink and X-Plane in one computer by using IP address (Bittar A., *et al.*, 2013). In this paper is not addressed in term of UDP in detail. It has been discussed by Hakiki, 2020.

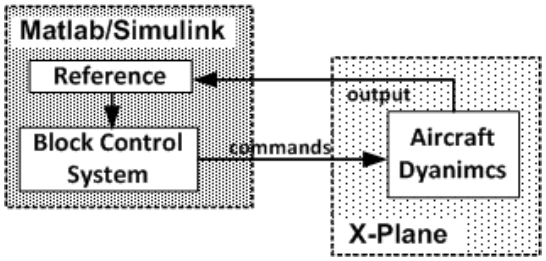

Figure 2-2 : Block diagram construction

2.1 Simulation Parameters

The setting angle of the rocket booster to longitudinal axis has the same angle size as the flight elevation angle of 18°. The launcher is modeled as a landing gear which is a skids type gear (Laminar Research, 2013), as shown in Figure 2-3. The simulation is conducted by varying the selected moment arms referring to the references (Shandi and Hakiki, 2016). The selected moment arms are shown in Table 2-1. A positive sign indicates that the CG point lies above the thrust line of the rocket. Otherwise, a negative sign indicates that the CG point lies below the line of thrust of the rocket.

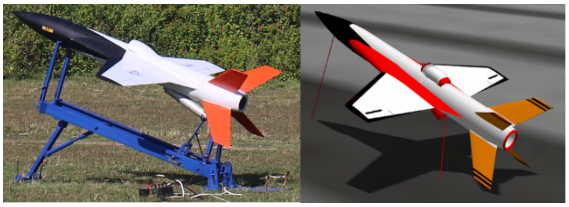

Figure 2-3 : Display RKX200TJ/booster

Table 2-1 : Data of mass and size of arm Moment

Vehicle Types	Total Mass (kg)	Moment Arm, d_{arm} (cm)
W_{CG1}	30.5	2.87
W_{CG2}	29.2	1.32
W_{CG3}	29.4	-1.91
W_{CG4}	25.8	0.4

2.2 Design of Control System

The designed pitch control system aim to maintain and control the pitch disturbances during a booster and climb phases. Whereas the roll control system keeps wing symmetrical wing position (wing leveler).

The configuration of the pitch control system is used, as shown in Figure 2-4. This system has three loops. Outer loop is in the feedback pitch angle (θ_c) and there are two inner loops, namely the pitch damper and the feedback elevator deflection. The pitch damper system is implemented to increase the damping ratio of the pitch oscillation mode (Hakiki, 2020). The pitch angle reference (θ_{ref}) and the angle θ_c pass through the comparator, resulting in an error signal (θ_e). This is then multiplied by the controller's pitch gain (θ_{gain}), yielding the input for the pitch damper system block. Signal ($\Delta\theta$) and signal (q), which is amplified by the pitch rate gain (q_{gain}), are compared to produce an elevator deflection signal ($\Delta\delta_e$). This signal is added to the feedback elevator deflection signal (δ_{ec}), obtaining a new elevator deflection position (δ_e), as shown in Figure 2-4 (Bittar, *et al.*, 2013), (Hakiki, 2020).

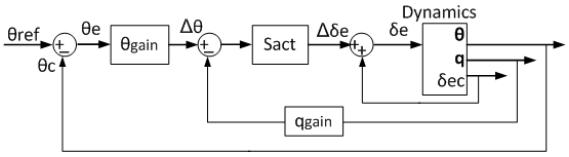

Figure 2-4 : Pitch control block diagram

Control system block diagram is responsible to maintain wing leveler, as shown in Figure 2-5. The roll damper helps to improve the effect of artificial increase in wingspan. The roll mode can also influence the aircraft's trajectory by causing a delay of the time when a turn is commanded (Peters and Konyak, 2012). Block Diagram is shown Figure 2-5 indicates that the signal (ϕ_e) is deviation between the reference *roll* (ϕ_{ref}) and the current *roll* (ϕ_c). The signal is ehnanced with the roll signal gain (ϕ_{gain}) to become signal Δp. The servomotor for moving the deflection of aileron is generated from the ratio of the signal Δp to the feedback angular velocity signal (p) which is amplified by the roll rate gain (p_{gain}) (Bittar, *et al.*, 2013), (Hakiki, 2020).

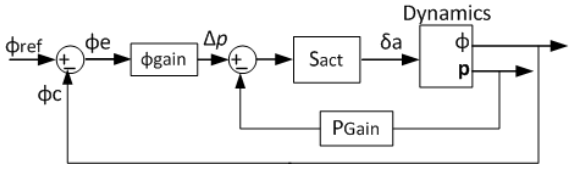

Figure 2-5 : Block diagram of roll control

The control system chosen is PID. To get the PID control feedback effect on the system motion by varying the gain value (Purwanto, *et al., 2013*). In this research, the PID coefficient is obtained based on trial and error. S_{act} is a transfer function for actuators. The transfer function is represented as a first-order system as seen in equation 2-1. τ is a time constant , which is set to 0.1 s (Nelson, 1998).

$$S_{act} = \frac{1}{\tau s+1} \qquad (2\text{-}1)$$

3 Result dan Analysis

The simulation conducted at two flight condition, that is :

a. Ballistic flight.
   The vehicle is pushed by a single rocket booster which has an average mass and thrust of 3 kg and 150 kgf, respectively. It has a burn time of about 1.2 s.
b. Flight by control system.
   During the booster phase, θ_{ref} is adjusted according to the flight elevation angle. θ_{ref} is set at 5° to the climb phase. After the rocket booster phase, the turbo jet engine

(sustainer) acts as a propulsion in the next phase. The sustainer is idled prior to take-off.

3.1 Ballistic Flight

The three flight parameters indicate that the vehicle is statically stable but the only one is instability. Stability of the vehicle can be seen from the response to the changes in the pitch angle (θ), the roll angle (ϕ), angle of attack (α) and side-slip angle (β) as shown in Figure 3-1, Figure 3-2, Figure 3-3, and Figure 3-4. Whereas Figure 3-5 and Figure 3-6 illustrate the aircraft flight performance.

The first case (d_{arm1}) which refers to Table 2-1, the vehicle experiences a pitch-up where the change in θ reaches 86° for 1.8 s, as shown in Figure 3-1. The vehicle tends to be unstable. The vehicle even experiences a pull-up accompanied by rolling movement, such as showing a spiral motion or the starting of a wobbling motion. The graph is shown in Figure 3-2 indicates that the change in ϕ reaches -180° in 1.4 s, followed by a roll movement of +180° at the 2nd second so that it causes a spiral motion. The other graph can also be seen the change in α during the first 1.8 s. The change in α occurs from 5° at 0.4 s to 25° at 1.4 s, as shown in Figure 3-3. The vehicle experiences a loss of lift or a stall at the 1.4 s in this regime. Overall, the change in β decreases and tends to move stable after the first second. It does not really affect the vehicle dynamics, except at the 6.6th second where there is the change in β by -8°. The vehicle experiences instability in the initial phase so that it affects its flight path further as shown in Figure 3-6.

The change in θ reaches 71° within 1.5 s occurs in the second flight condition (d_{arm2}), as shown in Figure 3-1. Once the rocket booster has burned out, the vehicle is quite stable. Because the static stability range is still fulfilled so that it can restore its attitude towards the disturbance direction. The changes in ϕ, α and β tend to be stable, as shown in Figure 3-2, Figure 3-3, and Figure 3-4, so that the flight path is according to its azimuth direction, as seen in Figure 3-6. The altitude and range of the vehicle are 126.8 m and 173.3 m, respectively, whereas the flight time is 11.6 s. The range calculation can be seen on the reference (Jan-Philip, 2010).

The next variation of the moment arm (d_{arm3}), the vehicle tends to move a pitch-down until the change in θ reaches -5° within 1.2 s, as shown in Figure 3-1. Despite returning to pitch up, the vehicle has lost its lift. Range and altitude are quite short about 66.4 m in 2.8 s with and 3.65 m, respectively, as shown in Figure 3-6. The angles of ϕ, α, and β are stable tendency, as shown in Figure 3-2, Figure 3-3, and Figure 3-4.

In last variant, the vehicle flies very stable although the angle θ rises to 36°, as shown in Figure 3-1. The other motion responses also indicate that the vehicle is stable. The rocket booster thrust can push the vehicle achieving nearly 250 m for 9.2 s while altitude approaches 78 m, as shown in Figure 3-6.

The flight speed profiles generally show the same pattern characteristics, as seen in Figure 3-5. There are differences of velocity which is affected by the difference in the mass of the vehicle, the angle θ and the moment arm size. The effect of θ indicates that the great pitch angle comes low velocity. The pitch angle effect is related to the gravity factor. The greatest velocity occurs on a vehicle with a moment arm (d_{arm3}) of 61.2 m/s, followed by d_{arm4}, d_{arm2}, and d_{arm1}, respectively, are 56.7 m/s, 49 m/s and 43 m/s. The last one, shows the

vehicle speed in unstable conditions. At 1.4 s, a stall occurs when the angle α reaches 25° and the velocity of about 36 m/s.

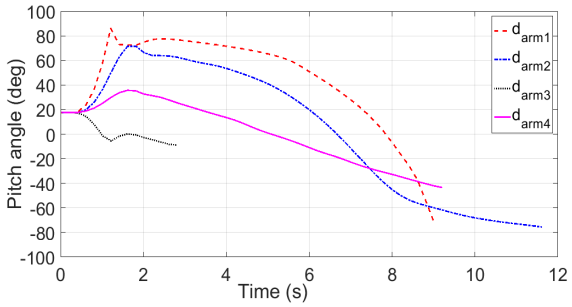

Figure 3-1 : Pitch angle response

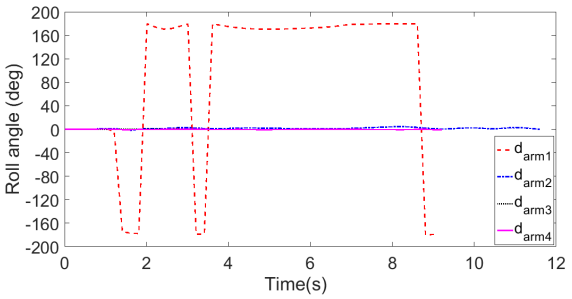

Figure 3-2 : Roll angle response

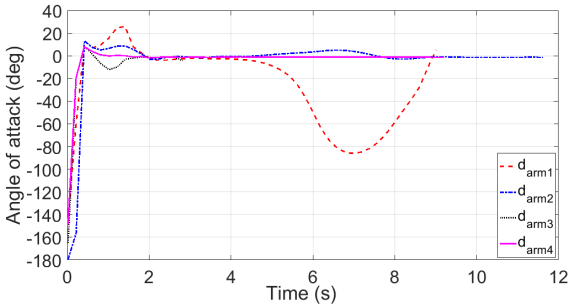

Figure 3-3 : Angle of attack response

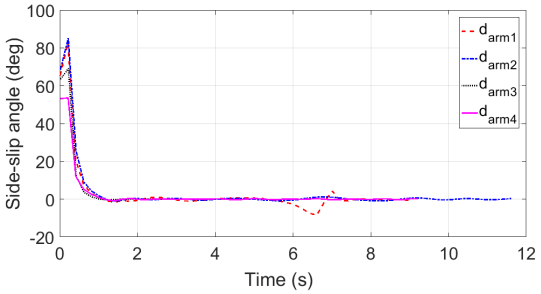

Figure 3-4 : Side-slip angle response

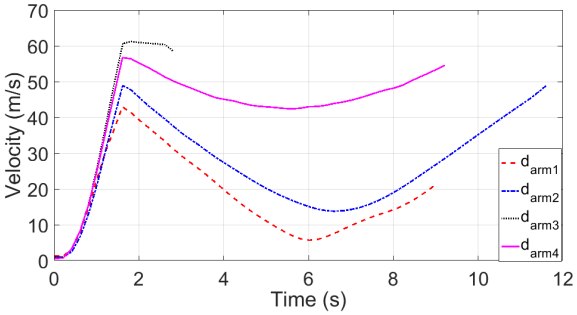

Figure 3-5 : Velocity profile

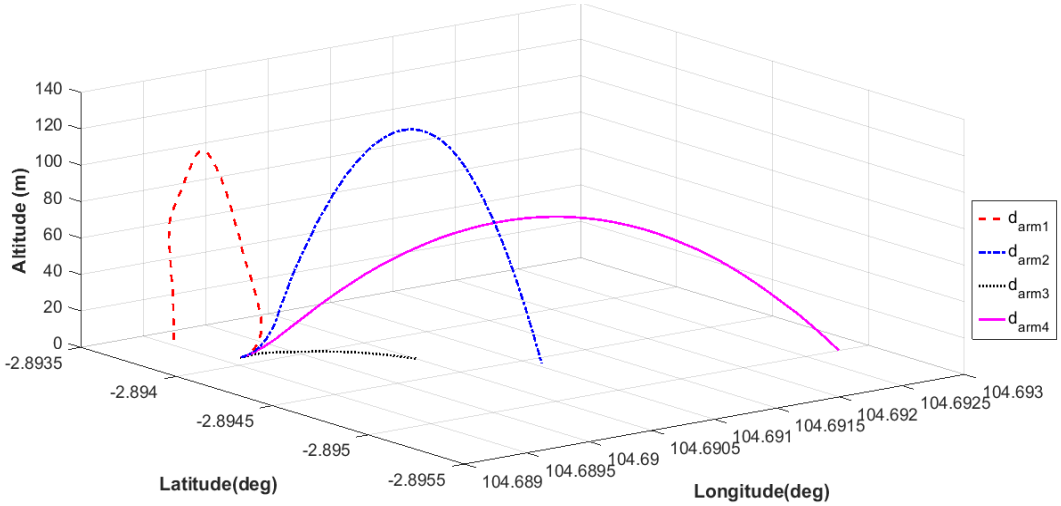

Figure 3-6 : Trajectory of ballistic flight

3.2. Flight by Control System

The PID coefficient values are selected as shown in Table 3-1. Overall, the control system manage to control the vehicle well, except the case of d_{arm1}.

Table 3-1 : The PID Coefficient chosen

Gain Controller	P	I	D
θ_{gain}	-0.3	0	0.1
q_{gain}	-0.1	0	0.15
φ_{gain}	-0.1	0	0
p_{gain}	0	0	0.1

In the case of d_{arm1}, the stability disturbance is large enough so that the vehicle is quite difficult to control parameters of θ and ϕ in the first 10 s as shown in Figure 3-7 and Figure 3-8. Since parameters of θ and ϕ are disrupted, the other parameters also are disturbed such as angles α and β. The control system can stabilize the parameters of θ and ϕ subsequently. In the second flight condition (d_{arm2}), the pitch angle can be reduced from 71° in ballistic flight to 56°. The pitch angle control further manages to maintain the angle of 5° with a settling time of 2.8 s. In the third case, the angle θ can be reduced to -1.5° for 1.2 s, while a settling time is 2.8 s next phase. The latter case, the angle θ can be damped a 27% drop compared to the ballistic phase. Settling time even is faster than others by 2.5 s.

During the autopilot phase, the lateral disturbance can be well damped, as shown in Figure 3-8, except the case of d_{arm1}. In contrast to the response of angle α, the disturbance occurs at the beginning of the rocket booster phase. After the 5th second, the angle α is adequately stable, as shown in Figure 3-9. The change in the angle θ affects the angle α and the flight path angle so that it can be altered its trajectory. Overall, the response of the angle β is stable, as shown in Figure 3-10.

The flight speeds in the case of d_{arm1}, d_{arm2}, d_{arm3}, and d_{arm4}, respectively, were 41 m/s, 50 m/s, 57 m/s and 54 m/s as shown in Figure 3-11. There are value difference of flight speed occurs between the autopilot phase and ballistic flight after the rocket booster is burned out. This difference is due to the effect of drag on the deflected control plane and the change in the angle α. The flight parameter (d_{arm4}), there is a disturbance after the 16th second, but it was still within a reasonable limit of stability, as shown in Figure 3-7, although this disturbance slightly affects the vehicle flight speed, as seen in Figure 3-11.

The cases of d_{arm2}, d_{arm3}, and d_{arm4} indicate that the trajectory corresponds to the azimuth angle by 113° North. In contrast, there is a flight path deviation which the case of d_{arm1} strays around 90° to the azimuth angle, as shown in Figures 3-12 and 3-13.

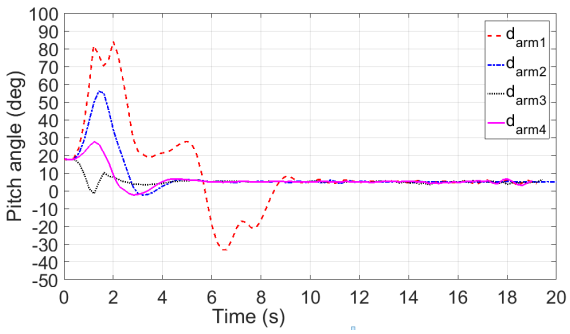

Figure 3-7 : Response of the change in θ

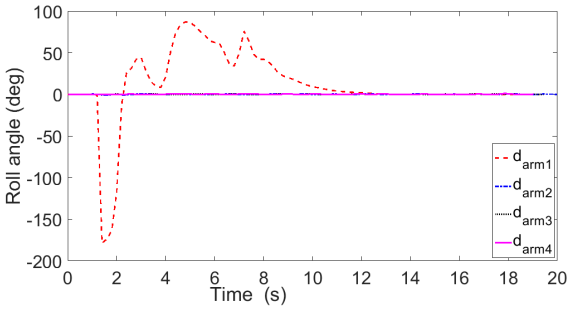

Figure 3-8 : Response of the change in ϕ

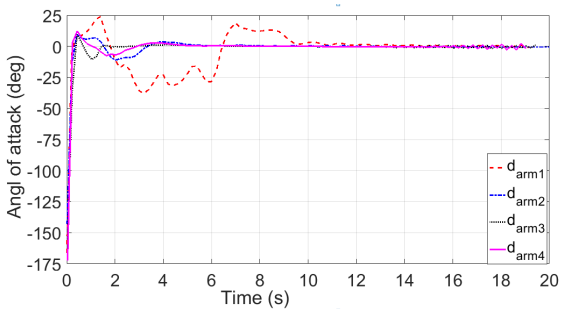

Figure 3-9 : Response of angle of attack change

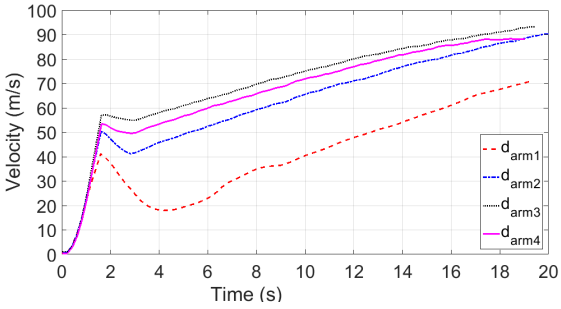

Figure 3-11 : Flight speed profile

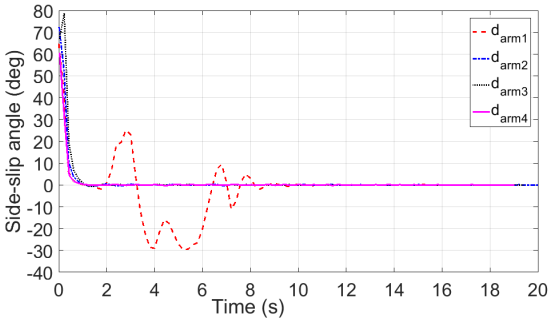

Figure 3-10 : Change in β response

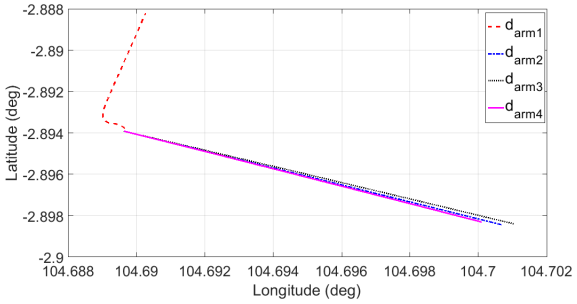

Figure 3-12 : A flight path in a geographiccoordinate system

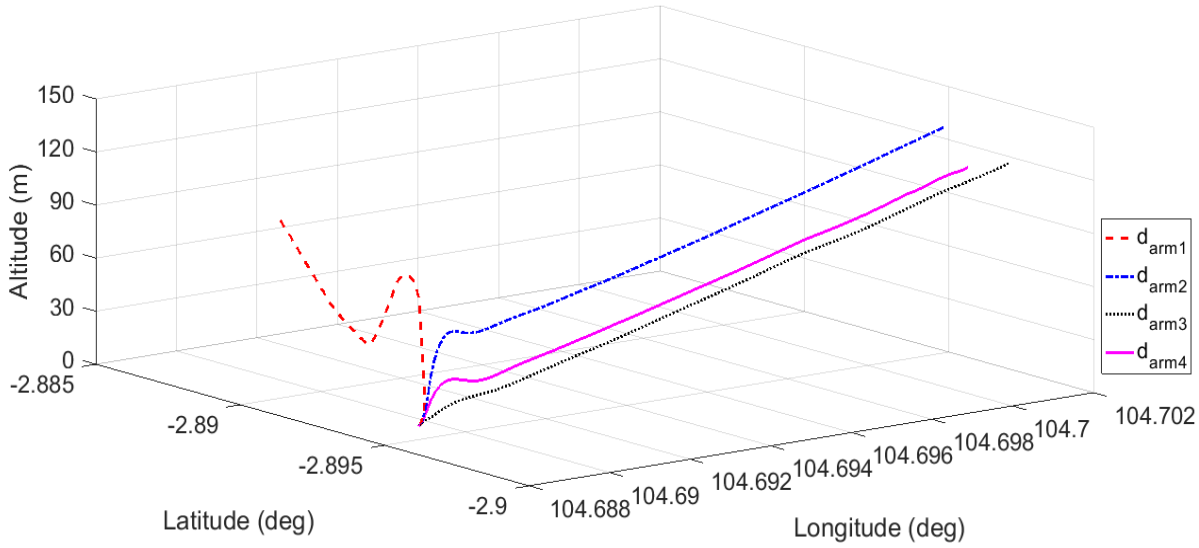

Figure 3-13 : Path flight

4 Conclusions

Overall, the control system which the PID coefficient value above indicates an overview of the characteristics of the vehicle controlled. Except, in the case of the moment arm (d_{arm1}) which shows static instability and uncontrollability during the rocket booster phase. The pitch control system can control parameter θ so that reduce the pitch angle increase of 21-27% and maintain the angle θ of 5°. While the roll control system can reduce lateral interference by maintaining the wing position at zero level ($\phi = 0$).

This paper provides conclusions and input for further design, namely the maximum limit of the moment arm value that is still feasible for the designed vehicle is 1.32 cm which the CG point lies above the thrust line of the booster.

Whereas the CG point lies below the thrust line of the booster is 1.9 cm.

Acknowledgements

The author want to express gratitude to the RKX200 teammates of the Rocket Technology Center, LAPAN, whom they have developed RKX-200TJ/booster.

References

R. Austin, (2010), *Unmanned Aircraft Systems UAVS Design*, Development and Deployment, John Wiley & Sons Ltd, Great Britain, pp. 35–43.

Hakiki, (2020), *Research on Co-Simulation of Flying for an Unmanned Aerial Vehicle (UAV)*, Keimyung University, South of Korea.

Lorenz Meier, Petri Tanskanen, Friedrich Fraundorfer, Marc Pollefeys, (2011), *PIXHAWK: A system for autonomous flight using onboard computer vision*, Proceedings - IEEE International Conference on Robotics and Automation May 2011, DOI: 10.1109/ICRA.2011.5980229.

Satrya, E., Riyadl, A., Sudiana, O., Hakiki., Sofyan, E., (2014). *Proses Perancangan Wahana RKX 200-EDF*, Hasil Penelitian Dan Pemikiran Ilmiah Tentang Teknologi Pesawat Terbang, Tangerang.

Hakiki., Sofyan, E., (2013), *Controlling X-Plane Flight Simulator Environments From Matlab For RKX-EDF Launch Scenario*, Proceedings International Seminar Of Aerospace Science And Technology 17th SIPTEKGAN, Tangerang.

Riyadl, Hakiki, (2014), *Pengaruh Momen Akibat Gaya Dorong Roket Booster Pada Dinamika Terbang Wahana RKX-200TJ : Studi Kasus Pada saat Take-off*, pp 196-203 , SIPTEKGAN XVIII, Rumpin

Shandi, Hakiki, (2016), *Prediksi letak pusat Gravitasi RKX-200TJ/Booster*, pp 57-64, SIPTEKGAN XX 2016 Rumpin Bogor 2016

Bo Liu, Zhou Fang, Ping Li and Chuanchuan Hao, (2011), *Takeoff analysis and simulation of a small scaled UAV with a rocket booster*, Advanced Materials Research Vol 267 (2011) pp 674-682 ©(2011) Trans Tech Publications, Switzerland,doi:10.4028/www.scientific.net/AMR.267.674

Riyadl, (2015), *Pengaruh dari Posisi Pusat Massa Roket yang tidak Terletak pada Sumbu Axis Simetri Terhadap Dinamika Terbang Roket Balistik, pp 139-148 – Journal of Aerospace Technology vol 13 December 2015 ISSN 1412-8063.*

Kaviyarasu, A., and Senthil, K. K., (2014), *Simulation of Flapping-wing Unmanned Aerial Vehicle using X-plane and Matlab/Simulink*, *Defence Science Journal*, 64(4), pp. 327-331. DOI: 10.14429/dsj.64.4933.

Bittar A.; Oliveira N., (2013), *Central*

Processing Unit for An Autopilot : Description and Hardware-In-the-Loop Simulation Autopilot. In Journal of Intelligent and Robotic Systems, April 2013, pp. 557–574. DOI 10.1007/s10846-012-9745-y.

Laminar Research, (2013), "*Plane Maker for X-Plane 10*,"

Eko B. Purwanto, Sufendi Lie, Syahron H. Nasution, 2013, *Pemodelan dan Simulasi Sistem Kendali Proportional Integral Derivative untuk Kestabilan Dinamika Terbang*, Majalah Sains dan Teknologi Dirgantara Vol. 8 No. 2, 48-59.

Peters, M., and Konyak, M. A., (2012), *The Engineering Analysis and Design of the Aircraft Dynamics Model For the FAA Target Generation Facility*, Final Report, Simulation Branch and Laboratory Services Division, Atlantic City, pp. 17–20.

Nelson, R. C., (1998), *Flight Stability and Automatic Control*, 2nd ed., McGraw-Hill New York, pp. 210–215.

Matuscheck, Jan-Philip, (2010), *Finding Points Within a Distance of a Latitude/Longitude Using Bounding Coordinates*, from http://janmatuschek.de/LatitudeLongitudeBoundingCoordinates diakses pada 29 April 2019.